Progress In Electromagnetics Research, PIER 102, 197–211, 2010

EMBEDDED ANTENNAS IN DRY AND SATURATED CONCRETE FOR APPLICATION IN WIRELESS SENSORS

X. Jin and M. Ali

Department of Electrical Engineering
University of South Carolina
Columbia, SC 29208, USA

Abstract—Efficient embedded antennas are needed for future wireless structural health monitoring. The input return loss and transmission losses of a dipole, a planar inverted-F antenna (PIFA), a microstrip patch, and a loop antenna are studied at around 2.45 GHz when these antennas are embedded inside a concrete cylinder. Antenna performance is investigated in free-space, in air dried concrete and in saturated concrete with and without the presence of steel reinforcements. It is observed that the maximum transmission loss for a distance of 250 mm between antennas is around 50 dB which is acceptable for inside the bridge wireless communication between sensors.

1. INTRODUCTION

The infrastructure that supports the smooth operation of our society such as, buildings, roads, bridges and stadiums has grown in an incredible rate during the last decades. Many of these structures have surpassed their life cycle and require routine structural evaluation to ensure proper operation and safety. Structural Health Monitoring (SHM) focuses on developing sensor technologies and systems that assess the integrity of structures (strain, corrosion etc.) such as buildings, bridges, and aero-space structures. Apart from conventional visual inspection [1] and ground penetrating radar (GPR) [2, 3] various types of sensors have been introduced for SHM applications, such as fiber optics [4], strain gauges [5], accelerometers, guided wave [6] and ultra sound sensors. Such sensors and the necessary wire connections must be installed while the infrastructure is being built. The wires

Corresponding author: M. Ali (alimo@cec.sc.edu).

connect the sensors with their data acquisition stations to which measured data are collected and processed. More recently there has been a growing interest on wireless sensors for structural health monitoring [7, 8]. Assessing the condition of the steel reinforcement inside concrete is not easy, since the steel is typically buried beneath one inch or more of concrete. In that case wireless sensors can be embedded inside concrete during the construction phase of the infrastructure. Such a sensor will contain a sensing element (strain sensor), a wireless transceiver, and one or more antennas. If the embedded sensor has a battery it must also be replenished from outside when needed. Thus one must know how antenna performance will change as they are embedded in concrete in order to design miniature efficient antennas for integration with wireless sensors. In [9] the characteristics of a microstrip patch antenna was investigated at 2.4 GHz when the antenna was embedded within concrete. In our research group studies on the characteristics of an embedded microstrip patch antenna at 2.45 GHz were performed [10–12]. In [13] the prospects of beaming wireless power to an antenna embedded inside concrete was studied at 5.7 GHz.

The goal of this paper is to investigate the return loss, transmission loss, gain, and radiation patterns of a number of well known antenna structures when embedded inside concrete. We specifically focus on a bridge pier and envision that wireless sensors will be embedded inside it. Each wireless sensor will consist of a sensing element and a wireless transceiver to send and receive data. The operation will be in a sleep/wake mode according to a defined schedule. To enable effective communication among buried sensors themselves as well as between a sensor and an outside base station we need to know how to design efficient communication antennas that can function inside concrete and steel reinforcements in the presence of variable quantities of moisture. We must also know the extent of the power loss such antennas will experience once embedded.

The paper is organized as follows. Firstly, since knowing the dielectric constants and conductivity of concrete is a must before any antenna is modeled using a full-wave electromagnetic solver, such as HFSS, we perform a literature review of the dielectric constant and conductivity of concrete. Secondly, we perform HFSS simulations of pairs of buried dipole, loop, microstrip patch, and planar inverted-F antennas inside two scale models of a concrete bridge pier. Finally, we analyze the resonance properties of each kind of antenna and the transmission loss between two antennas of the same kind considering air-dried concrete, saturated concrete, and reinforced air-dried and saturated concrete. We primarily focus our study around the 2.45 GHz

frequency due to the easy availability of miniature wireless transceiver modules at this frequency.

2. DIELECTRIC PROPERTIES OF CONCRETE

To design efficient embedded antennas for a bridge pier, we need to know the relative permittivity (dielectric constant) and conductivity of concrete. It is well known that the propagation of electromagnetic waves will be affected by the presence of moisture in the concrete. The higher the moisture content the stronger will be the effect. The dielectric constant is very sensitive to the moisture content in concrete. The complex permittivity of concrete varies with both the frequency and the moisture content. At any given frequency both dielectric constant and conductivity increase as moisture content increases [14–18]. For several moisture contents, [19–22] give analytical results of dielectric constant of concrete as function of frequency. In [23, 24] the relationship between the moisture content of concrete and the measured amplitude attenuation of radio waves were studied at 1.5 GHz (which showed the corresponding microwave power loss). In [23–26] the permittivity of reinforced concrete with metal mesh/gird or steel bars buried inside and its relationship with respect to the moisture content, frequency, and physical location of the metal objects were studied. Buyukozturk [18] measured and provided the dielectric constant, loss factor, and conductivity of concrete from 0.1 GHz to 20 GHz for four different moisture content values: wet, saturated, air dried, and oven dried. Such values for saturated and air dried concrete at 2.45 GHz are listed in Table 1. These were the parameters we used in our HFSS simulations. The term saturated means that there is significantly higher moisture inside the concrete. According to [18] concrete specimens were cast with a ratio of water to cement, sand, and coarse aggregate mix of 1 : 2.22 : 5.61 : 7.12 (by weight). The age of the specimens was 4 weeks at the time of the measurements. Saturated specimens had 6.27% gravimetric water content (by weight) and air dried concrete was very close to almost dry. Wet specimen

Table 1. Measured permittivity of concrete at 2.45 GHz [18].

	Air Dried	Saturated	Air
Dielectric Constant, ε_r	4.5	8.1	1.0006
Conductivity, σ	0.013	0.13	0
Loss Tangent, $\tan(\delta)$	0.0212	0.1178	0

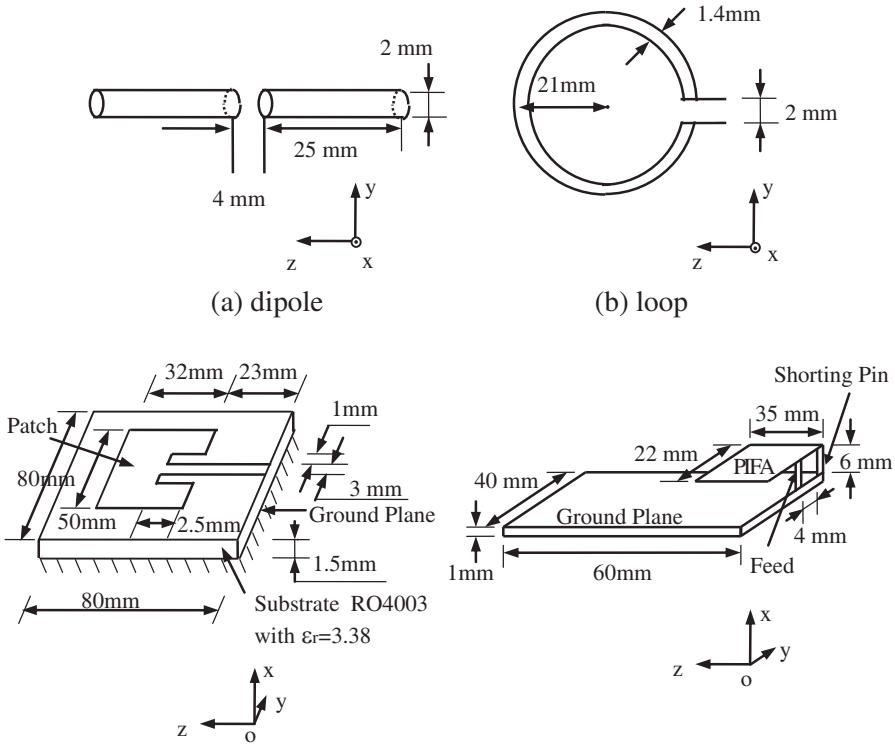

Figure 1. Geometrical dimensions of the antennas under consideration: (a) Dipole, (b) loop, (c) microstrip patch, and (d) PIFA.

had a watery surface, saturated specimen had moisture only inside, and air dried specimen was exposed to ambient room temperature and humidity. From [18], we obtained the loss tangent data using $\tan(\delta) = \sigma/(\varepsilon_r \varepsilon_0 \omega)$, where ω is angular frequency.

3. GEOMETRY AND COMPUTATIONAL DETAILS

To investigate the return loss, transmission loss, gain and pattern of antennas buried inside a concrete pier a dipole, a loop, a microstrip patch, and a planar inverted-F antenna (PIFA) were designed for operation at 2.45 GHz in free space. The geometry and dimensions of these antennas are given in Fig. 1. Two cases of embedding scenarios were considered: Case 1 — A concrete cylinder without steel rebars and

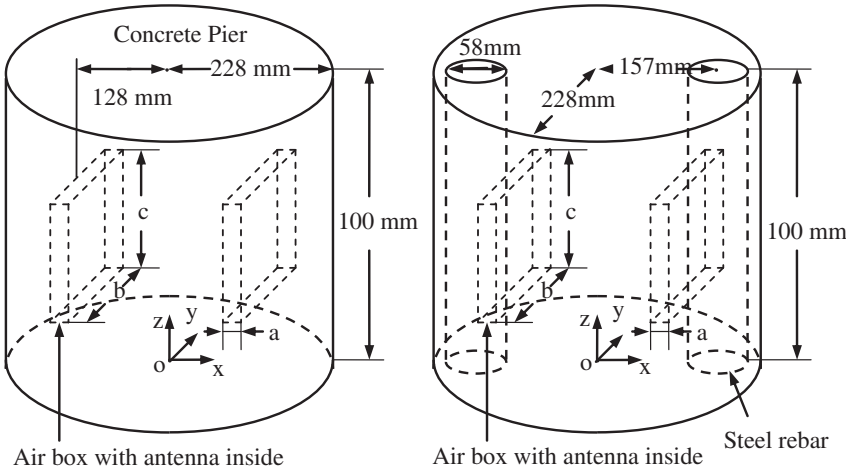

(a) Case 1 (b) Case 2

Figure 2. The HFSS models in (a) concrete and in (b) reinforced concrete.

Table 2. Dimensions of the air boxes that contain the antennas and distances.

Antenna Type	a (mm)	b (mm)	c (mm)	r (mm)	d (mm)
Dipole	5	5	80	245	5
Loop	6	50	50	244	5.3
Patch	6	86	86	250	2.4
PIFA	14	46	66	243	3

Case 2 — A concrete cylinder with steel rebars. Fig. 2(a) represents Case 1 while Fig. 2(b) represents Case 2. For simplicity and ease of simulation a cylindrical concrete pier of 100 mm height and 228 mm radius was considered. We consider that two antennas each of the same kind are placed inside air boxes with dimensions a, b and c. Each antenna is oriented along the z-axis which is also the axis of the cylindrical concrete pier. The farthest side of each air box is 128 mm away from the center axis of the pier. The two antenna scenario described here represents a transmit-receive system inside a bridge pier. The dimensions of the air box (a, b and c) for each antenna are given in Table 2. The distances r between the antennas and the distances d between the antennas and the nearby surface of the steel rebar are also given in Table 2.

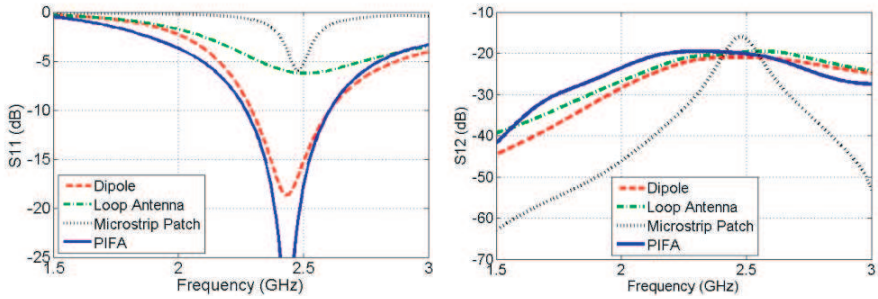

Figure 3. Computed return loss (S_{11}) and transmission (S_{12}) data for all antennas in free space.

4. RETURN LOSS AND TRANSMISSION LOSS

4.1. Antennas in Free Space

Simulated return loss (S_{11}) and transmission (S_{12}) plots for all antennas in free space are shown in Fig. 3. For each case two antennas of the same kind were placed at a distance of r from each other. The values of the parameter r are listed in Table 2.

From Fig. 3(a), it can be seen that the PIFA, the dipole, and the microstrip patch have resonances at 2.43, 2.42 and 2.48 GHz. Their corresponding bandwidths are 13.9, 13.1 and zero, respectively within -10 dB return loss. The patch exhibits an additional resonance at 3.25 GHz which is not shown here. The patch was tuned properly for operation inside concrete so it off tuned in free-space. The resonant frequency of the loop antenna is near 2.45 GHz. The loop has poor return loss at resonance because its input impedance is larger than the characteristic impedance of the feed transmission line (50 Ω). Computed transmission data between two antennas of each kind in free space are shown in Fig. 3(b). Only the transmission data near the antenna resonant frequencies are of interest here. The transmission between two dipoles, two loops, and two PIFAs is about -21 dB at their respective resonant frequencies. Only the microstrip patch has a transmission of -16 dB because of its higher gain.

4.2. Antennas in Concrete

The effects of concrete loading (consisting of different moisture contents) on antenna performance were studied. Fig. 4 shows the

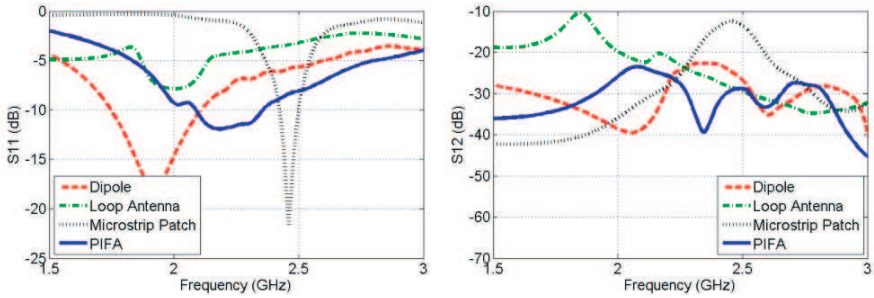

Figure 4. Computed return loss (S_{11}) and transmission (S_{12}) data of the antennas in air dried concrete.

simulated results for the dipole, loop, microstrip patch, and PIFA when embedded in air dried concrete.

When embedded in air dried concrete the resonant frequencies of the PIFA and the dipole decreased from their free space values of 2.43 and 2.42 GHz to 2.18 and 1.92 GHz, respectively. The dielectric loading presented by the air dried concrete is responsible for this. Since the air box (a, b) containing the dipole is small it allows smaller gaps between the sides of the dipole and the nearby concrete. This is why the dipole suffered a larger reduction in its resonant frequency. The same is also true for the loop whose resonant frequency decreased from 2.45 GHz to about 2.0 GHz. Conversely the PIFA has a larger (4 mm) air clearance on top of it (see Table 2) which results in a lesser reduction in its resonant frequency. The only antenna whose resonant frequency remained nearly unchanged is the microstrip patch. This is so because the patch radiates primarily through the fringing electric fields between the patch and the ground plane. Since there are no fields on top of the patch that contribute to the radiation the air gap on top of the patch is sufficient to keep it immune from any change in its resonant frequency.

The concrete loading affected the bandwidth of the dipole antenna the most, which increased from 13.1% in free space to 18.65% in air dried concrete. The bandwidth of the PIFA decreased to 12.1% in air dried concrete from 13.1% in free space. The bandwidth of the patch is 3.25%. Computed transmission (S_{12}) data between two antennas of each kind in air dried concrete are shown in Fig. 4(b). For dipoles the transmission data is between -40 and -32 dB within the dipole operating frequency band of 1.75 to 2.11 GHz. Transmission at resonance is -36 dB. Thus the worst case transmission loss between

two dipoles at resonance and in air dried concrete is 19 dB worse than that in free-space. Similarly for PIFAs the transmission data is between −40 and −24 dB within the PIFA operating frequency band of 2.09 to 2.36 GHz. Transmission at resonance is −25.4 dB. Same as the dipoles the worst case transmission loss between two PIFAs at resonance and in air dried concrete is 19 dB worse than that in free-space. The transmission between two loops at resonance and in air dried concrete is −20 dB which is about the same as the free-space transmission loss between two loops. The lower losses between the two loops in air dried concrete results from a much stronger mutual coupling between the two loops in this scenario. The transmission between two patches at resonance (2.45 GHz) in air dried concrete is about −12.5 dB. As explained before the smaller transmission loss between the two patches is due to the directional nature of the patch antennas.

Simulated return loss and transmission loss data for the same antennas in saturated concrete are shown in Fig. 5. From Table 1 the dielectric constant of air dried concrete and saturated concrete are 4.5 and 8.1, respectively. This increase in dielectric constant is expected to have an effect on the resonant frequencies of the antennas. As before the resonant frequencies of the dipole and the loop were affected the most.

The dipole and the loop resonant frequencies are 1.86 and 1.75 GHz, which are 3.1% and 12.9% lower than their resonant frequencies in air dried concrete. Also the bandwidth of the dipole in saturated concrete is 25.4% as opposed to its 18.65% bandwidth in air dried concrete. The bandwidth of the loop in saturated concrete is 2.9%. The PIFA resonates at 2.17 GHz while the patch resonates at 2.46 GHz. The bandwidth of the PIFA decreased (5.5%) due

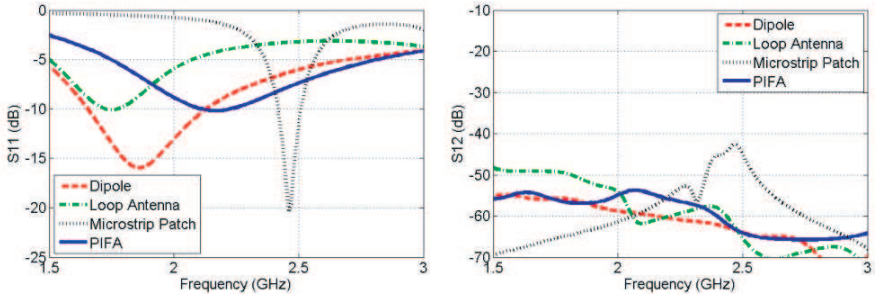

(a) (b)

Figure 5. Computed return loss (S_{11}) and transmission (S_{12}) data of the antennas in saturated concrete.

to a degradation in the antenna impedance matching which can be easily corrected by adjusting the feed to shorting pin distance. The bandwidth of the patch is 3.65%, slightly larger than 3.25% in air dried concrete.

Computed transmission data between two antennas of each kind in saturated concrete for are shown in Fig. 5(b). For dipoles the transmission data is between −60 and −55 dB within the dipole operating frequency band of 1.65 to 2.13 GHz. For the loops the transmission data is −50 dB within the loop's very narrow operating frequency band of 1.73 to 1.78 GHz. For PIFAs the transmission loss is −55 dB at resonance. For the patchs the transmission data is −43 dB at resonance and between −46 and −43 dB within the operating frequency band of 2.42 to 2.51 GHz. The worst case transmissions one may expect between two antennas in saturated concrete are −60 dB, −50 dB, and −55 dB and −46 dB for dipoles, loops, and PIFAs and patches, respectively. These are 20 dB, 30 dB, 15 dB, and 33.5 dB in saturated concrete than that in air dried concrete.

4.3. Antennas in Reinforced Concrete

A simplified model of a bridge pier consisting of two steel reinforcements is shown in Fig. 1(b). The dipoles, loops, PIFAs, and patches were placed next to the steel reinforcement and simulated using HFSS. Computed return loss and transmission data for all four types of the antennas are shown in Fig. 6, where the distance of each antenna from the nearby steel rebar is shown in Table 2.

The presence of the steel rebar in close proximity deteriorates the dipole return loss significantly. This is because dipole antennas

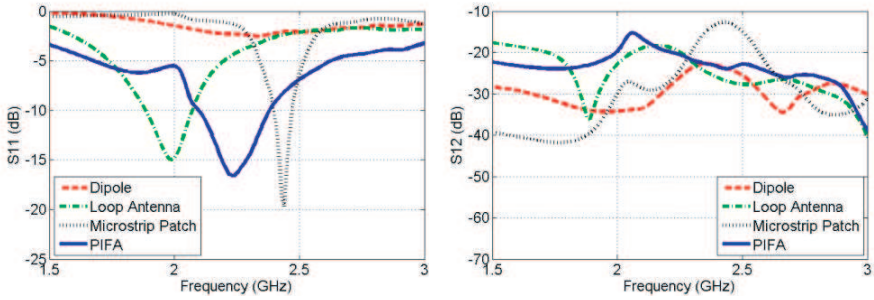

(a) (b)

Figure 6. Computed return loss (S_{11}) and transmission (S_{12}) data of the antennas, in air dried reinforced concrete.

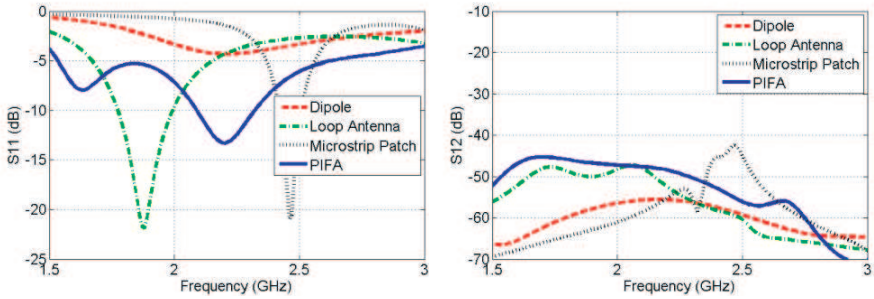

(a) (b)

Figure 7. Computed return loss (S_{11}) and transmission (S_{12}) data of the antennas, in saturated reinforced concrete.

Table 3. Characteristics of the dipole, loop, patch, and PIFA in free-space.

Antenna	In Free-Space				
	f_r	G_θ	G_φ	S_{11}	BW
Dipole	2.42	2.3	−54.2	−18.5	13.1
Loop	2.50	−1.1	2.6	−6.3	None
Patch	2.48	5.9	−3.9	−6.0	None
PIFA	2.43	3.9	2.2	−36.7	13.9

require larger separation from nearby metallic structures. The PIFA and the loop both have well defined resonances with good return loss characteristics. Their resonant frequencies are 2.23 GHz and 1.99 GHz, respectively. The bandwidths of the PIFA and the loop are 13% and 9.1%, respectively. The transmission loss between two PIFAs inside reinforced air dried concrete is between 20 to 24 dB for within the frequency band of 2.09 to 2.38 GHz. The transmission loss between two loops is between 20 to 35 dB within the frequency band of 1.89 to 2.07 GHz. The transmission loss between two patches is about 13 dB within the frequency band of 2.40 to 2.47 GHz. The loop and the PIFA inside reinforced saturated concrete show slightly lower resonant frequencies while the transmission loss ranges between 48 to 50 dB for the PIFA and 48 to 50 dB for the loop. The transmission loss for the patch is about 43 dB at resonance.

Table 4. Characteristics of the dipole, loop, patch, and PIFA in concrete.

Antenna	In Air Dried Concrete					In Saturated Concrete				
	f_r	G_θ	G_φ	S_{11}	BW	f_r	G_θ	G_φ	S_{11}	BW
Dipole	1.92	−2.0	−11.5	−17.9	18.65	1.86	−15.6	−25.6	−16.0	25.4
Loop	2.01	−1.9	3.7	−7.9	None	1.75	−17.3	−13.6	−10.1	2.9
Patch	2.46	3.6	−6.2	−21.6	3.25	2.46	−16.9	−19.6	−20.4	3.65
PIFA	2.18	1.5	1.6	−11.9	12.1	2.17	−12.8	−14.5	−10.2	5.5

Table 5. Characteristics of the dipole, loop, patch, and PIFA in reinforced concrete.

Antenna	In Air Dried Reinforced Concrete					In Saturated Reinforced Concrete				
	f_r	G_θ	G_φ	S_{11}	BW	f_r	G_θ	G_φ	S_{11}	BW
Dipole	2.34	0.3	−12.6	−2.5	None	2.20	−33.2	−35.3	−4.3	None
Loop	1.99	−7.2	2.3	−15.0	9.1	1.88	−23.1	−18.4	−21.9	11.7
Patch	2.45	3.6	−7.0	−19.7	2.9	2.46	−16.5	−18.0	−21.0	3.65
PIFA	2.23	3.1	−2.1	−16.6	13.0	2.47	−12.7	−13.5	−13.3	10.4

5. GAIN AND PATTERNS IN CONCRETE

Characteristics of the dipole, loop, patch, and PIFA in free-space, in concrete, and in reinforced concrete are presented in Tables 3, 4, and 5. The symbols, f_r, G_θ and G_ϕ represent the resonant frequency in GHz, the theta component of the peak realized gain in dBi and the phi component of the peak realized gain in dBi, respectively. The symbol S_{11} represents the S_{11} in dB at the resonant frequency. BW represents bandwidth in percent.

Since the PIFA performed well in all of the scenarios described, computed normalized radiation patterns of the PIFA embedded inside the bridge pier are shown in Fig. 8. The patterns were normalized to the PIFA peak gain considering all cases and all planes. The desired angle of transmission is θ=90°. All of these patterns were computed at 2.45 GHz. Clearly the xz-plane pattern for the antenna in air dried concrete resembles the patterns of a monopole antenna on a finite ground plane. One interesting difference is that unlike a conventional monopole pattern with only one component of field the embedded PIFA has two components of field which are nearly similar in strength. As expected the patterns in saturated concrete and saturated reinforced

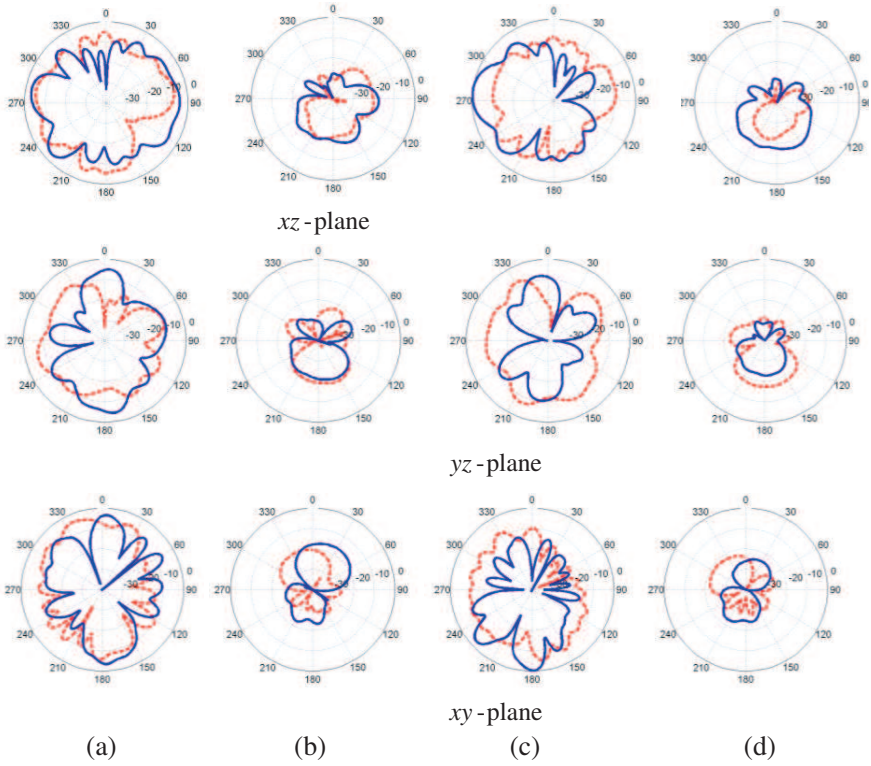

Figure 8. Computed normalized radiation patterns in (dB) of the PIFA in (a) air dried, (b) saturated, (c) air dried reinforced, and (d) saturated reinforced concrete. Solid — E_θ component and dotted — E_ϕ component.

concrete are much weaker than the patterns in air dried reinforced concrete.

6. CONCLUSION

The prospects of using embedded antennas inside concrete for wireless communication are investigated. Our study of a dipole, a microstrip patch, a loop, and a planar inverted-F antenna inside the model of a bridge pier show important guidelines for future embedded antenna design. Comparing antenna performance inside air dried and saturated concrete and with steel reinforcements it is found that both the planar inverted-F antenna and the microstrip patch will be good candidates for such applications. Although the loop antenna shows reasonably

good performance it requires larger space compared to the other antennas and will degrade in performance as more steel reinforcements are added. Similarly, the microstrip patch will also require larger space than the PIFA. As apparent, transmission loss for the PIFAs inside saturated concrete is around 45 to 48 dB. These data illustrate the feasibility of sensor to sensor data communication when the sensors are embedded inside a bridge pier. Either the PIFA or the patch has to be so designed that each is conformal to the rebar surface. Clearly these antennas if miniaturized can be used with RFIDs or individual distributed sensor nodes.

ACKNOWLEDGMENT

This work was supported in part by the National Science Foundation grant ECCS: 0619253.

REFERENCES

1. Moore, M., D. Rolander, B. Graybeal, B. Phares, and G. Washer, "Highway bridge inspection: State of the practice survey," *Federal Highway Administration*, Mc Lean, VA FHWA-RD-01-033, Apr. 2001.
2. Maierhofer, C., "Nondestructive evaluation of concrete infrastructure with ground penetrating radar," *Journal of Materials in Civil Engineering*, Vol. 15, No. 3, 287–297, May–Jun. 2003.
3. Ground Penetrating Radar, http://www.geosphereinc.com/gpr_gpradar.html.
4. Schulz, W. L., J. P. Conte, and E. Udd, "Long gauge fiber optic bragggrating strain sensors to monitor civil structures," *SPIE*, Vol. 4330, 56, 2001. http://www.bluerr.com/papers/BRR-2001_SPIE_Vol4330_p56.pdf.
5. Nagayama, T., M. R. Sandoval, B. F. Spencer, Jr., K. A. Mechitov, and G. Agha, "Wireless strain sensor development for civil infrastructure," http://osl.cs.uiuc.edu/docs/inss04nagayama/inss04nagayama.pdf.
6. Alleyne, D. N., B. Pavlakovic, M. J. S. Lowe, and P. Cawley, "Rapid long-range inspection of chemical plant pipework using guided waves," *Insight*, Vol. 43, 93–96, 2001.
7. Cho, S., C.-B. Yun, J. P. Lynch, A. Zimmerman, B. Spencer, Jr., and T. Nagayama, "Smart wireless sensor technology for structural health monitoring of civil structures," *International Journal of Steel Structures*, Vol. 8, No. 4, 267–275, KSSC, 2008.

8. Loh, K., J. P. Lynch, and N. A. Kotov, "Passive wireless sensing using SWNT-based multifunctional thin film patches," *International Journal for Applied Electromagnetics and Mechanics*, Vol. 28, No. 1–2, 87–94, IOS Press, 2009.
9. Bernhard, J. T., K. Hietpas, E. George, D. Kuchma, and H. Reis, "An interdisciplinary effort to develop a wireless embedded sensor system to monitor and assess corrosion in the tendons of prestressed concrete girders," *IEEE 2003 Topical Conference on Antennas for Wireless Communication*, Honolulu, Hawaii, 2003.
10. Shams, K. M. Z., M. Ali, and A. M. Miah, "Characteristics of an embedded microstrip patch antenna for wireless infrastructure health monitoring," *IEEE Antennas and Propagation Society International Symposium Digest*, Albuquerque, NM, Jul. 2006.
11. Shams, K. M. Z., A. M. Miah, and M. Ali, "Gain and transmission properties of an embedded microstrip patch antenna for structural health monitoring application," *IEEE Antennas and Propagation Society International Symposium*, Honolulu, Hawaii, Jun. 2007.
12. Shams, K. M. Z., *Novel Embedded Antennas and Engineered Materials for Wireless Communications and Sensing*, Ph.D. Dissertation, University of South Carolina, Sep. 2007.
13. Shams, K. M. Z. and M. Ali, "Wireless power transmission to a buried sensor in concrete," *IEEE Sensors Journal*, 1573–1577, Dec. 2007.
14. Shaaria, A., S. G. Millardb, and J. H. Bungeyb, "Modelling the propagation of a radar signal through concrete as a low-pass filter," *NDT & E International*, Vol. 37, 237–242, 2004.
15. Soutsos, M. N., J. H. Bungey, S. G. Millard, M. R. Shaw, and A. Patterson,, "Dielectric properties of concrete and their influence on radar testing," *NDT & E International*, Vol. 34, 419–425, 2001.
16. Tsui, F. and S. L. Matthews, "Analytical modeling of the dielectric properties of concrete for subsurface radar applications," *Construction and Building Materials,* Vol. 11, No. 3, 149–161, 1997.
17. Maierhofer, C. and J. Wostmann, "Investigation of dielectric properties of brick materials as a function of moisture and salt content using a microwave impulse technique at very high frequencies," *NDT & E International*, Vol. 31, No. 4, 259–263, 1998.
18. Buyukozturk, O., "Electromagnetic properties of concrete and their significance in nondestructive testing," *Transportation Research Record No. 1574, Advances in Concrete and Concrete*

Pavement Construction, 10–17, 1997.

19. Robert, A., "Dielectric permittivity of concrete between 50 MHz and 1 GHz and GPR measurements for building materials evaluation," *Journal of Applied Geophysics*, Vol. 40, 89–94, 1998.
20. Courtney, C., W. Motil, T. Bowen, and S. Blocher, "Measurement note 48: Measurement methods and the characterization of the electromagnetic properties of materials," Dec. 1996. http://www.ece.unm.edu/summa/notes/Measure/0048.pdf.
21. Sandrolini, L., U. Reggiani, and A. Ogunsola, "Modelling the electrical properties of concrete for shielding effectiveness prediction," *Journal Physics. D: Applied. Physics,* Vol. 40, 5366–5372, 2007.
22. Bourdi, T., J. E. Rhazi, F. Boone, and G. Ballivy, "Application of Jonscher model for the characterization of the dielectric permittivity of concrete," *IOP Publishing Journal of Physics D: Applied Physics*, Vol. 41, No. 20, 1–9, Oct. 21, 2008.
23. Laurens, S., M. E. Barrak, J. P. Balayssac, and J. Rhazi, "Aptitude of the near-field direct wave of ground-coupled radar antennas for the characterization of the concrete," *Construction and Building Materials,* Vol. 21, 2072–2077, 2007.
24. Sbarti, Z. M., "Effect of concrete moisture on radar signal amplitude," *ACI Materials Journal*, Nov.–Dec. 2006. http://findarticles.com/p/articles/mi_qa5360/is_200611/ai_n21404598/print?tag=artBody;col1.
25. Farr, E. G. and C. A. Frost, "Measurement notes, note 52: Impulse propagation measurements of the dielectric properties of water, dry sand, moist sand, and concrete," May 1997. http://www.farr-research.com/Papers/mn52.pdf.
26. Sbartai, Z. M., S. Laurens, J.-P. Balayssac, G. Arliguie, and G. Ballivy, "Ability of the direct wave of radar ground-coupled antenna for NDT of concrete structures," *NDT & E International*, Vol. 39, 400–407, 2006.